

New Journal of Chemistry

Supporting Information

MoS₂-based composite nanozymes with superior peroxidase-like activity for ultrasensitive SERS detection of glucose

Yaoyu Tan, Huan Jiang, Baihui Wang, Xia Zhang*

School of Materials Engineering, Shanghai University of Engineering Science,
Shanghai, 201620, China

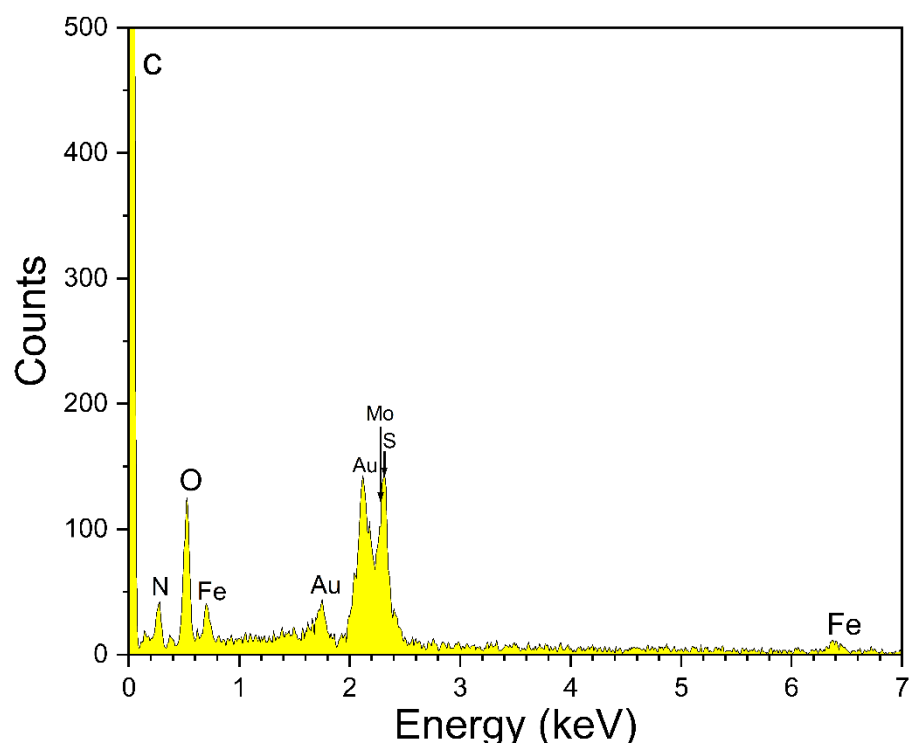


Figure S1. The EDS spectra of the PANI@MoS₂@Fe₃O₄@Au nanocomposites.

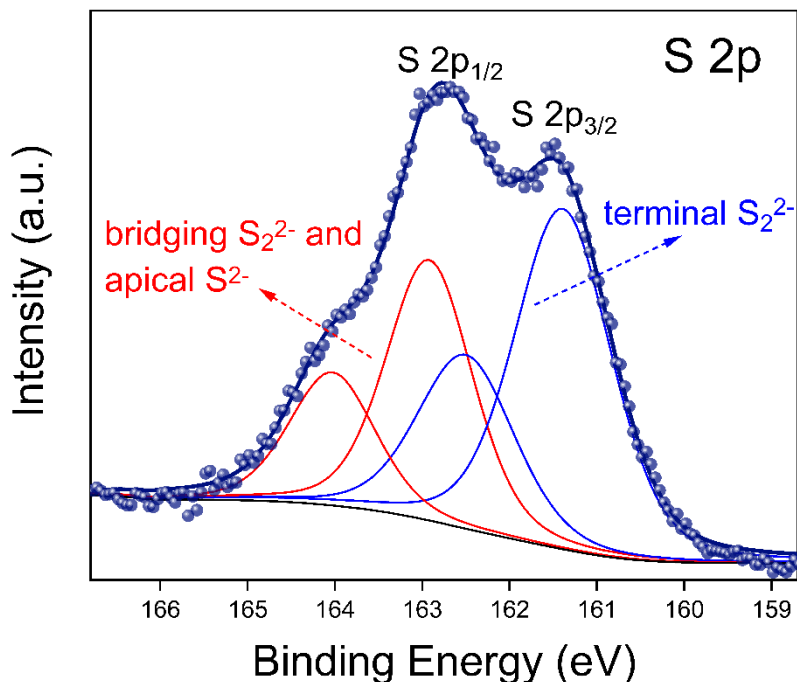


Figure S2. XPS spectra of S 2p of the PANI@MoS₂@Fe₃O₄@Au nanozymes.

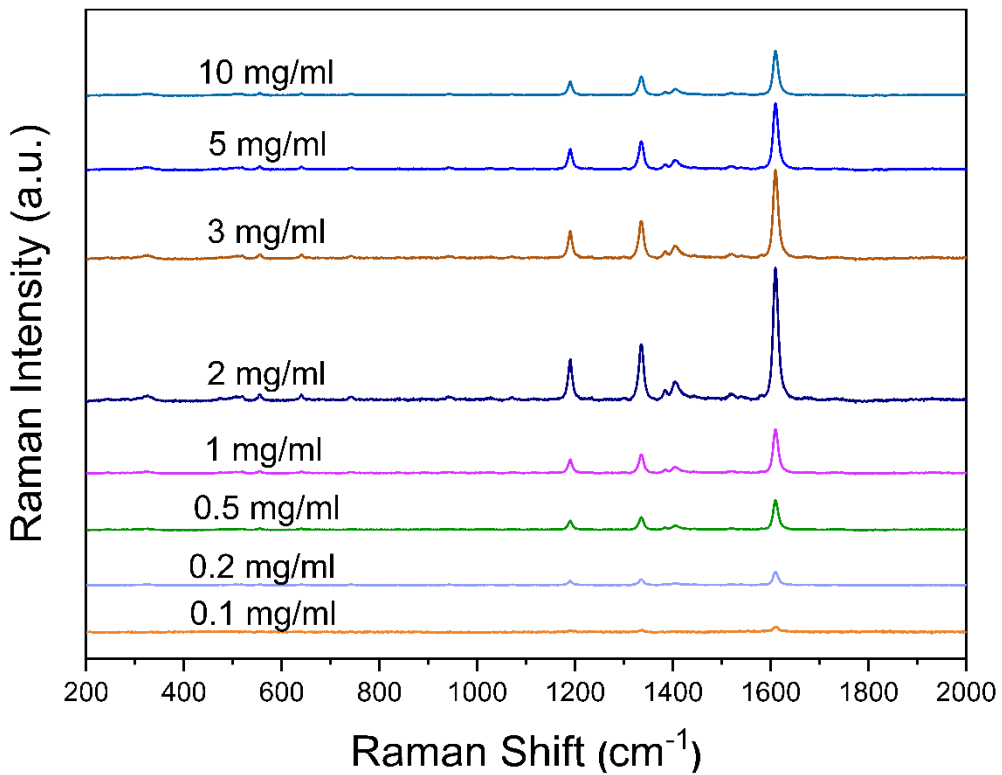


Figure S3. The SERS spectra of TMB molecules during the reaction on the surface of PANI@MoS₂@Fe₃O₄@Au nanozymes prepared at different concentrations of HAuCl₄. [PANI@MoS₂@Fe₃O₄@Au] = 10 μL (100 μg·mL⁻¹); [TMB] = 10 μL (1 mM); [H₂O₂] = 10 μL (10⁻⁵ M).

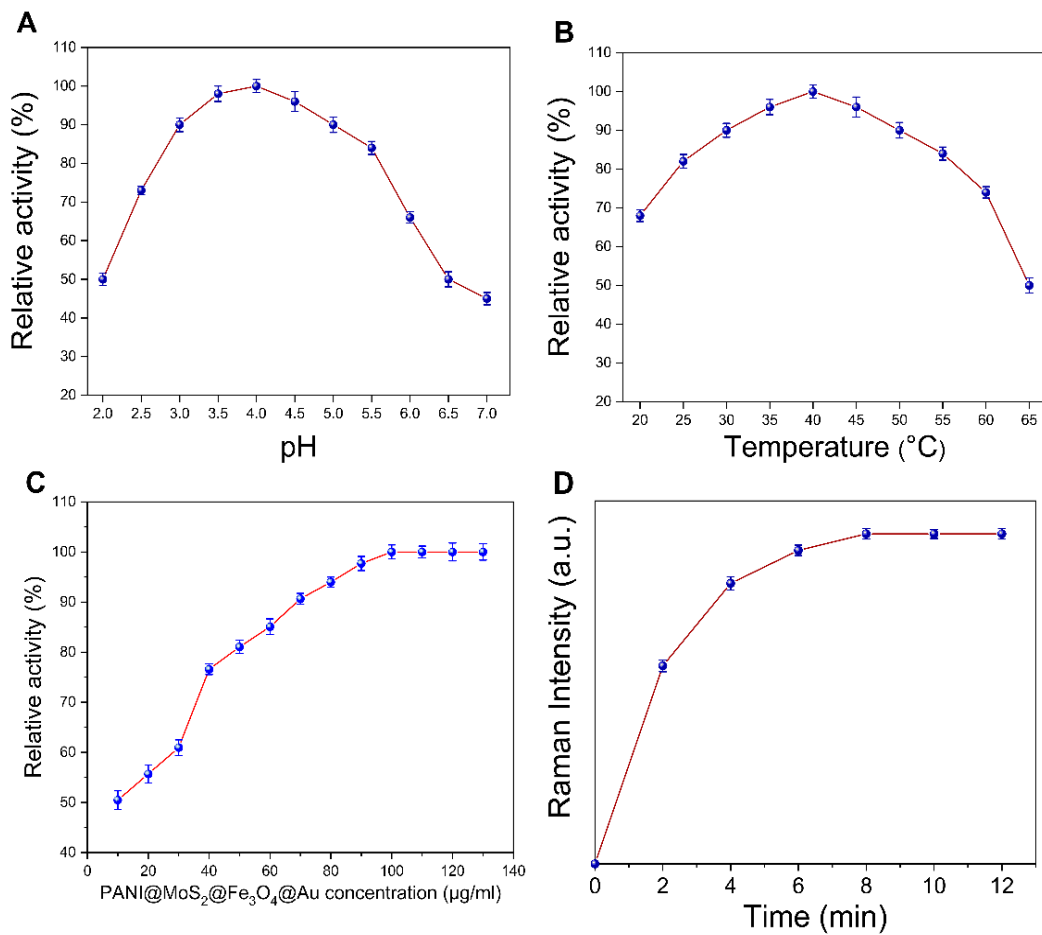


Figure S4. Peroxidase activities under varied reaction conditions. (A) A pH-dependent response curve is performed at pH 2.0-7.0. (B) Temperature (20°C, 25°C, 30°C, 35°C, 40°C, 45°C, 50°C, 55°C, 60°C, 65°C). (C) Effect of PANI@MoS₂@Fe₃O₄@Au concentration on catalytic efficiency (10, 20, 30, 40, 50, 60, 70, 80, 90, 100, 110, 120, 130 mg·mL⁻¹), and (C) Dependence of the peroxidase-like activity on time (0, 2, 4, 6, 8, 10, 12 min). (D) System reaction changes with time (0, 2, 4, 6, 8, 10, 12 min). Error bars represent the standard error derived from three repeated measurements.

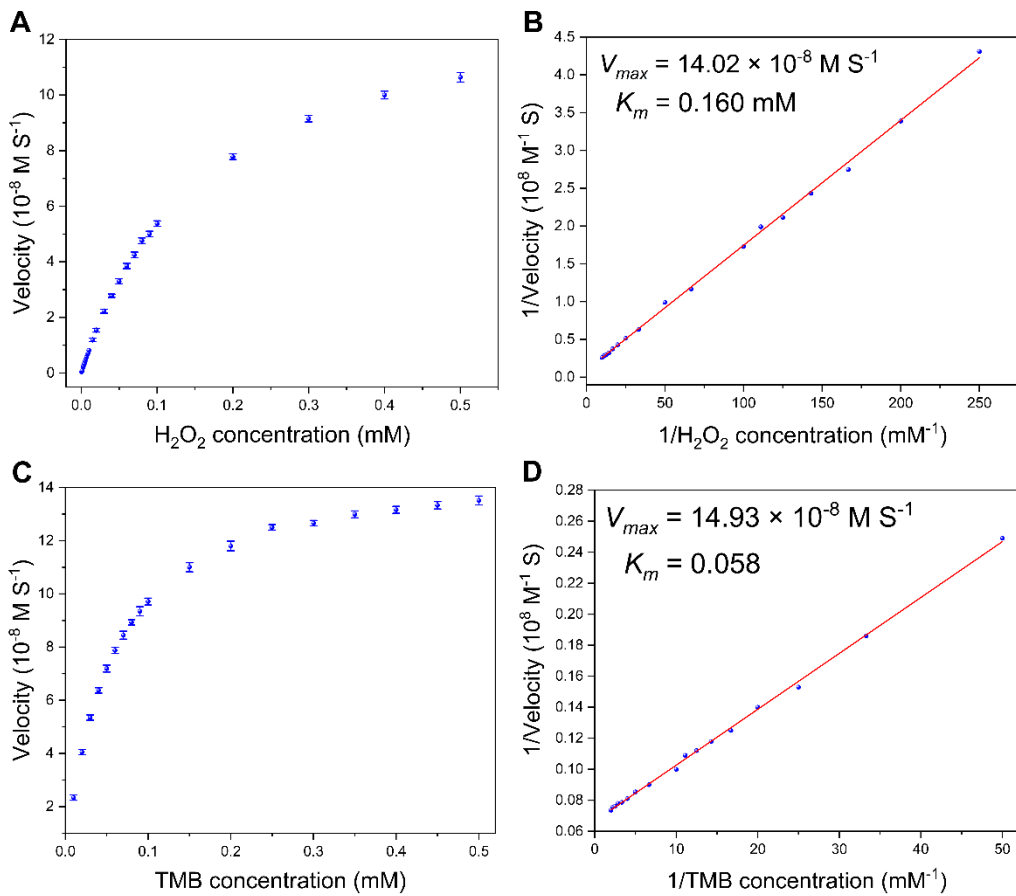


Figure S5. UV-vis-kinetic assays of the PANI@MoS₂@Fe₃O₄@Au nanozymes. (A) Plots of the velocity of the reaction versus different concentrations of H₂O₂ (0.5 mM TMB). (B) Lineweaver-Burk plots of the velocity versus varying concentration of H₂O₂. (C) Plots of the velocity of the reaction versus different concentrations of TMB (1 mM H₂O₂). (D) Lineweaver-Burk plots of the velocity versus varying concentration of TMB.

Table S1. Comparison of the kinetic parameters with natural enzyme and other nanocatalysts.

Nanocatalysts	Substrates	K_m (mM)	V_{max} ($10^{-8} \text{ M}\cdot\text{s}^{-1}$)	Ref.
HRP	TMB	0.434	10.0	1
	H ₂ O ₂	3.7	8.71	
Fe ₃ O ₄	TMB	0.098	3.44	1
	H ₂ O ₂	154	9.78	
MoS ₂	TMB	2.668	1.501	2
	H ₂ O ₂	1.809	1.642	
NiFe ₂ O ₄	TMB	0.55	4.57	3
	H ₂ O ₂	2.6	14.11	
Fe ₂ O ₃ Mesoporous	TMB	0.298	7.36	4
	H ₂ O ₂	146.7	6.37	
CuO	TMB	25	10.49	5
	H ₂ O ₂	400	16.1	
Fe ₃ O ₄ @C	TMB	0.20	1.34	6
	H ₂ O ₂	0.23	2.41	
MoS ₂ @MgFe ₂ O ₄	TMB	0.806	141.3	7
	H ₂ O ₂	0.238	37.8	
GO-Fe ₃ O ₄	TMB	0.43	13.08	8
	H ₂ O ₂	0.71	5.31	
MoS ₂ -PPy-Pd	TMB	0.93	-	9
	H ₂ O ₂	6.4	-	
PANI@MoS ₂ @Fe ₃ O ₄ @Au	TMB	0.054	14.87	This work
	H ₂ O ₂	0.159	13.83	

Table S2. Comparisons of various nanomaterial-based biosensors for glucose.

Target	Detection techniques	Nanomaterial	Linear range	LOD	Ref.
glucose	VL	AuNPs-MWCNT-IL/GCE	5-120 μM	2 μM	¹⁰
glucose	FL	CeO ₂ NPs	10-200 μM	8.9 μM	¹¹
glucose	CL&SERS	Au@Ag NPs	0.5-400 μM	0.02 μM	¹²
glucose	EC	Ag NP-graphene	2000-1×10 ⁴ μM	100 μM	¹³
glucose	EC	Au NPs-CNTs/3DF	50-2000 μM	1.07 μM	¹⁴
glucose	SERS	PANI@MoS ₂ @Fe ₃ O ₄ @Au	10 ⁻⁵ -10 ³ μM	10 ⁻⁶ μM	this work

VL: Voltammetry. FL: Fluorimetry. CL: Colorimetry. SERS: Surface-enhanced Raman scattering. EC: Electrochemistry.

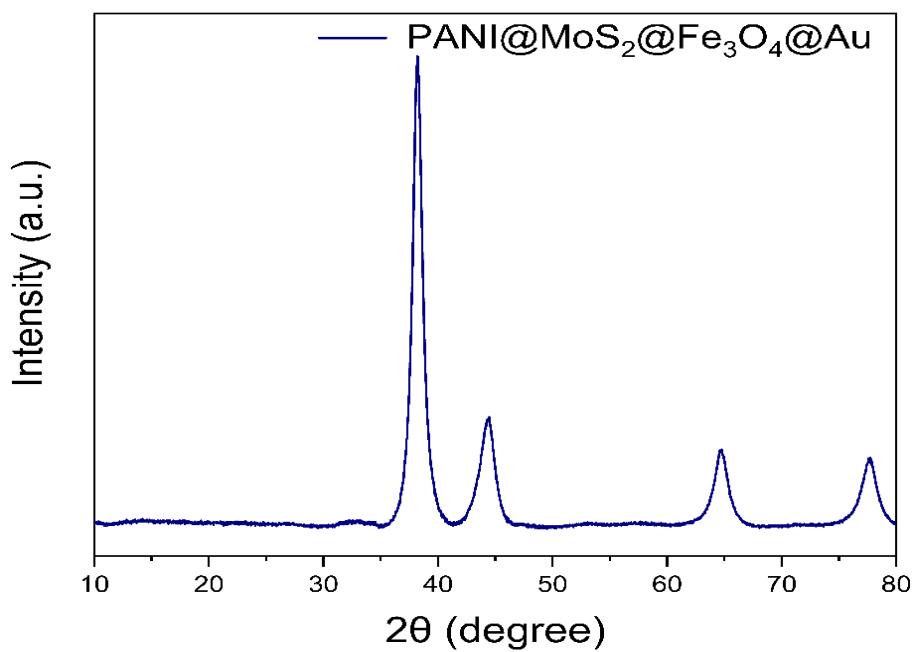
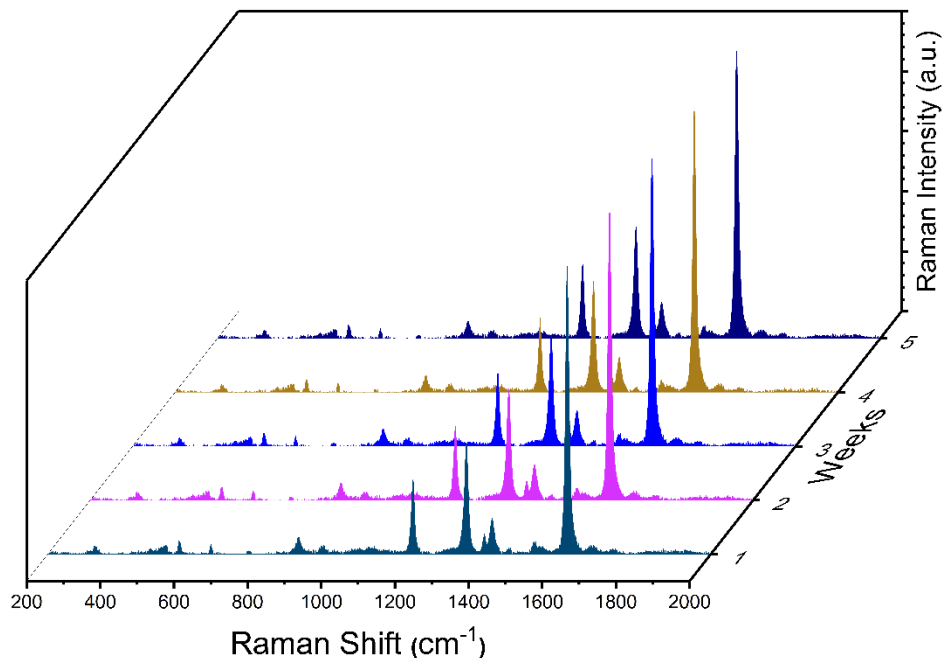
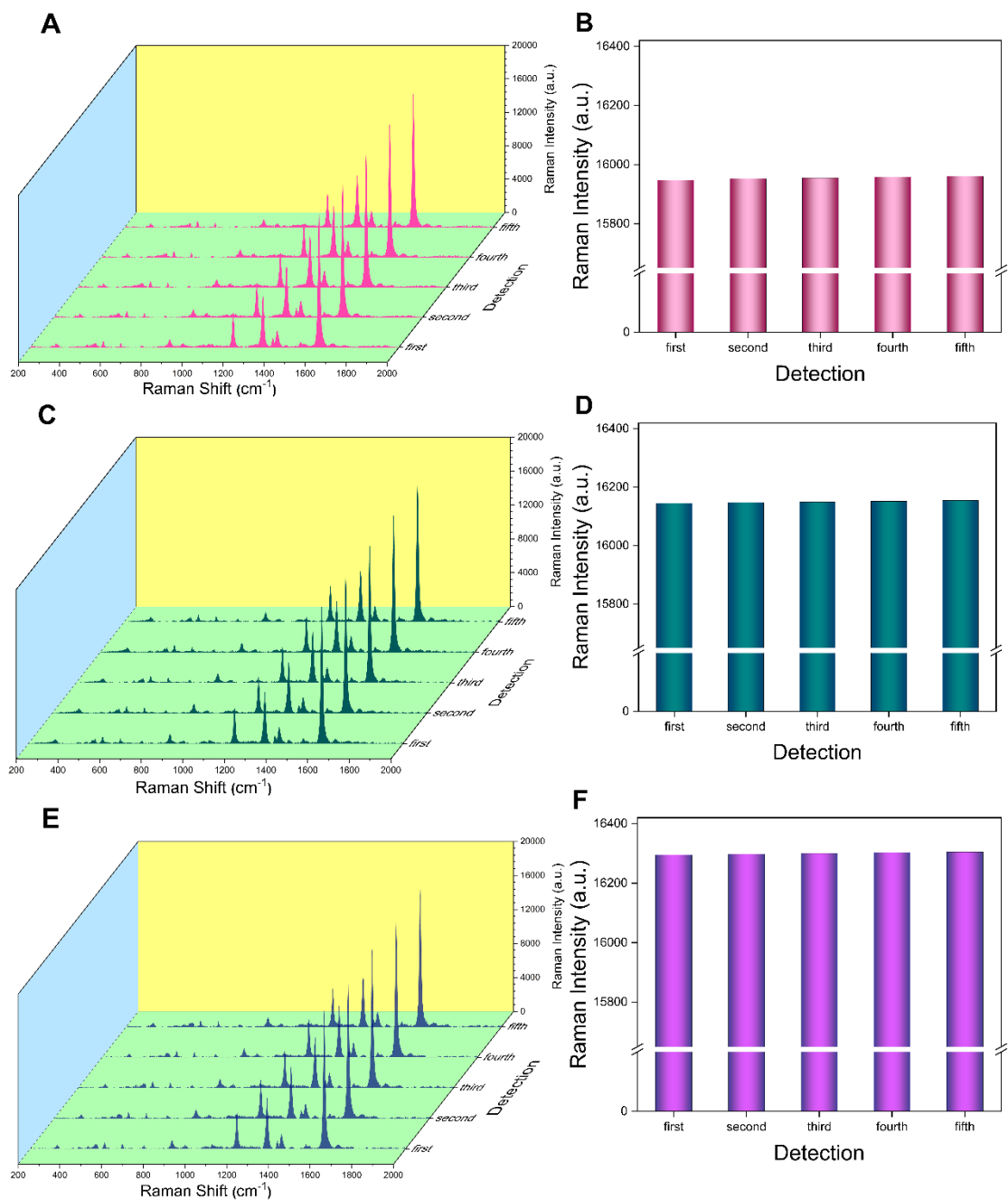


Figure S6. XRD patterns of PANI@MoS₂@Fe₃O₄@Au nanozyme after 7 days in PBS.



Firure S7. SERS spectra of glucose(10^{-5} M) determination of PANI@MoS₂@Fe₃O₄@Au nanozymes in 5 weeks.



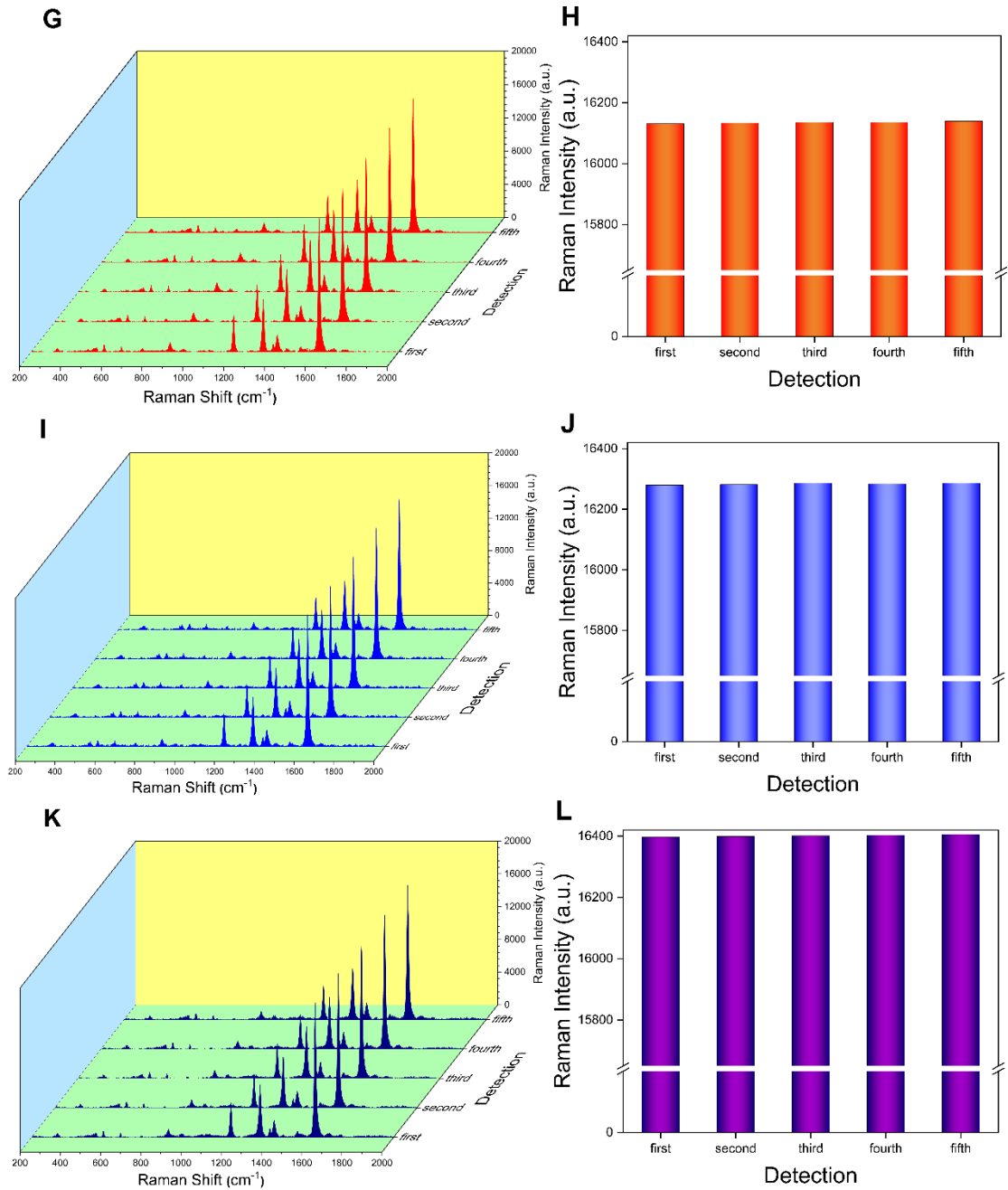


Figure S8. The Raman spectrum of the glucose content of human serum sample 1 after the addition of the value [(A) 2 mM, (C) 4 mM, (E) 6 mM] determined by the SERS method and the corresponding intensity histogram at 1609 cm^{-1} [(B) 2 mM, (D) 4 mM, (F) 6 mM]. Sample 1 is a human serum with a glucose concentration of 3.28 mM. The Raman spectrum of the glucose content of human serum sample 2 after the addition of the value [(G) 2 mM, (I) 4 mM, (K) 6 mM] determined by the SERS method and the corresponding intensity histogram at 1609 cm^{-1} [(H) 2 mM, (J) 4 mM, (L) 6 mM]. Sample 2 is a human serum with a glucose concentration of 5.12 mM.

Supporting References

1. L. Gao, J. Zhuang, L. Nie, J. Zhang, Y. Zhang, N. Gu, T. Wang, J. Feng, D. Yang, S. Perrett and X. Yan, *Nature Nanotechnology*, 2007, **2**, 577-583.
2. W. Dong, G. Chen, X. Hu, X. Zhang, W. Shi and Z. Fu, *Sensors and Actuators B: Chemical*, 2020, **305**, 127530: 127531-127510.
3. L. Su, W. Qin, H. Zhang, Z. U. Rahman, C. Ren, S. Ma and X. Chen, *Biosensors and Bioelectronics*, 2015, **63**, 384-391.
4. R. Bhattacharjee, S. Tanaka, S. Moriam, M. K. Masud, J. Lin, S. M. Alshehri, T. Ahamad, R. R. Salunkhe, N.-T. Nguyen, Y. Yamauchi, M. S. A. Hossain and M. J. A. Shiddiky, *Journal of Materials Chemistry B*, 2018, **6**, 4783-4791.
5. A. P. Nagvenkar and A. Gedanken, *ACS Applied Materials & Interfaces*, 2016, **8**, 22301-22308.
6. R. Zhang, N. Lu, J. Zhang, R. Yan, J. Li, L. Wang, N. Wang, M. Lv and M. Zhang, *Biosensors and Bioelectronics*, 2020, **150**, 111881: 111881-111889.
7. Y. Zhang, Z. Zhou, F. Wen, J. Tan, T. Peng, B. Luo, H. Wang and S. Yin, *Sensors and Actuators B: Chemical*, 2018, **275**, 155-162.
8. Y. l. Dong, H. g. Zhang, Z. U. Rahman, L. Su, X. j. Chen, J. Hu and X. g. Chen, *Nanoscale*, 2012, **4**, 3969-3976.
9. M. Chi, Y. Zhu, L. Jing, C. Wang and X. Lu, *Analytica Chimica Acta*, 2018, **1035**, 146-153.
10. H. Zhu, X. Lu, M. Li, Y. Shao and Z. Zhu, *Talanta*, 2009, **79**, 1446-1453.
11. B. Liu, Z. Sun, P. J. Huang and J. Liu, *Journal of the American Chemical Society*, 2015, **137**, 1290-1295.
12. Y. Zhong, X. Yu, W. Fu, Y. Chen, G. Shan and Y. Liu, *Microchimica Acta*, 2019, **186**, 802.
13. Y. Zhang, S. Liu, L. Wang, X. Qin, J. Tian, W. Lu, G. Chang and X. Sun, *RSC Advances*, 2012, **2**, 538-545.
14. L. G. Bach, M. L. N. Thi, Q. B. Bui and H. T. Nhac-Vu, *Materials Research Bulletin*, 2019, **118**, 110504.

